Increased Right Ventricular Septomarginal Trabeculation Mass is a Novel Marker for Pulmonary Hypertension

Comparison With Ventricular Mass Index and Right Ventricular Mass

Jens Vogel-Claussen, MD,†‡ Monda L. Shehata, MD,* Dirk Lossnitzer, MD,§ Jan Skrok, MD,* Sukhminder Singh, MD, MS,¶ Danielle Boyce, MPH,¶ Noah Lechtzin, MD, MHS,¶ Reda E. Girgis, MD,¶ Stephen C. Mathai, MD, MHS,¶ Joao A. Lima, MD,‖ David A. Bluemke, MD, PhD,** and Paul M. Hassoun, MD¶*

Objective: To prospectively evaluate the cardiac magnetic resonance (MR) imaging-derived measurement of right ventricular (RV) septomarginal trabeculation (SMT) mass as a noninvasive marker for pulmonary hypertension (PH), compared with the ventricular mass index (VMI = RV mass/left ventricular mass) and RV mass.

Materials and Methods: A total of 49 patients (60 ± 12 years; 35 female) with suspected PH underwent cardiac MR and right heart catheterization on the same day. Eighteen normal volunteers were also included. The performance of SMT mass, VMI and RV mass measurement, with regard to PH detection, was analyzed using receiver operating characteristic curves. Logistic regression analysis was used to assess the association between SMT mass, RV mass, VMI, and PH.

Results: The area under the receiver operating characteristic curve for SMT mass/body surface area (BSA), VMI, and RV mass/BSA in diagnosing the presence or absence of PH was 0.88, 0.87, and 0.73 respectively. In multivariable models, both SMT mass/BSA ($P = 0.005$, odds ratio: 8.6) and VMI ($P = 0.012$, odds ratio: 1.1) were found to be significant, independent predictors of PH.

Conclusion: Compared with right heart catheterization measurement, SMT mass and VMI are reproducible and noninvasive MR imaging markers for the diagnosis of PH.

Key Words: cardiac MRI, pulmonary hypertension, ventricular mass index, right ventricular septomarginal trabeculation

(*Invest Radiol* 2011;46: 567–575)

Pulmonary hypertension (PH) defined as a mean pulmonary arterial pressure greater than 25 mm Hg is a disease with high morbidity and mortality.[1,2] PH is usually suspected clinically based on symptoms, physical findings, and the results of screening Doppler echocardiography (DE), although a definitive diagnosis typically requires invasive right heart catheterization (RHC). Noninvasive assessment of pulmonary arterial pressure by DE is derived from estimation of the right ventricular systolic pressure after measurement of the tricuspid regurgitation peak velocity.[3,4] However, DE can be inaccurate with the possibility of over- or underestimating the presence and degree of PH. The latter can lead to significant delay in diagnosis of a potentially lethal disease. In addition, adequacy of DE for the diagnosis of PH may be substantially hindered by several conditions, such as the absence of a detectable jet of tricuspid regurgitation, a limited acoustic window (ie, due to advanced lung disease).[5–7]

In recent years, cardiac magnetic resonance (MR) imaging has become the reference standard modality for the evaluation of cardiac anatomy and function,[8] and new imaging markers for PH have emerged using this technique, including main pulmonary artery mean flow using phase contrast magnetic resonance imaging (MRI), the left ventricular (LV) septal to LV free wall curvature ratio, the ventricular mass index (VMI = RV mass/LV mass), and delayed enhancement at right ventricular (RV) attachment sites.[9–12]

The septomarginal trabeculation (SMT) near the anterior RV site is a muscular band that originates from the interventricular septum (IVS) at the lower segment of the crista supraventricularis, and forms a functional unit with the moderator band, which attaches to the lateral free wall and apex of the RV.[13,14] Strategically situated between the RV inflow and outflow tracts, the whole unit is thought to assist in emptying blood from the RV into the pulmonary trunk during systole. On the basis of our clinical observation that the RV SMT was frequently hypertrophied in patients with PH (Figs. 1A, B), we hypothesized that SMT remodeling could serve as a reliable marker of the disease should correlate with the degree of RV remodeling and hemodynamic changes. Although hypertrophy of the SMT-moderator band complex has been reported previously as a cause of subpulmonic stenosis in a case series of 17 patients,[15] it has only been associated with a single case of primary PH (currently known as idiopathic pulmonary arterial hypertension [IPAH]) without subpulmonic stenosis, as assessed by echocardiography.[16]

Therefore, the aim of our study was to prospectively evaluate the SMT mass as a potential imaging marker for PH and RV dysfunction. We also compared its performance as a novel marker to the VMI and RV mass, which are now established MR markers for PH.[9,17]

METHODS

Study Design

Between January 2007 and March 2009, a total of 51 patients who were referred for evaluation of clinically known or suspected PH were examined with cardiac MR and RHC, performed on the same day at 2 clinical centers (Johns Hopkins Hospital [n = 32], and Heidelberg University Hospital [n = 19]). This prospective study

Received November 17, 2010, and accepted for publication, after revision, March 14, 2011.

From the *Department of Radiology, Johns Hopkins University School of Medicine, Baltimore, MD; †Department of Diagnostic and Interventional Radiology, University Hospital Tuebingen, Tuebingen, Germany; ‡Department of Radiology, Hannover Medical School, Hannover, Germany; §Department of Cardiology, University Hospital Heidelberg, Heidelberg, Germany; ¶Division of Pulmonary and Critical Care Medicine, Department of Medicine, Johns Hopkins University School of Medicine, Baltimore, MD; and ‖Division of Cardiology, Johns Hopkins University School of Medicine, Baltimore, MD; and **Department of Radiology and Imaging Sciences, National Institutes of Health, National Institute of Biomedical Imaging and Biomedical Engineering, Bethesda, MD.

Conflicts of interest and sources of funding: NIH 1P50HL08946. DAB supported by the NIH intramural research program.

Reprints: Jens Vogel-Claussen, MD, Department of Radiology, Johns Hopkins University, Nelson Basement MRI 143, 600 N Wolfe St, Baltimore, MD 21287. E-mail: jclauss1@jhmi.edu.

ISSN: 0020-9996/11/4609-0567

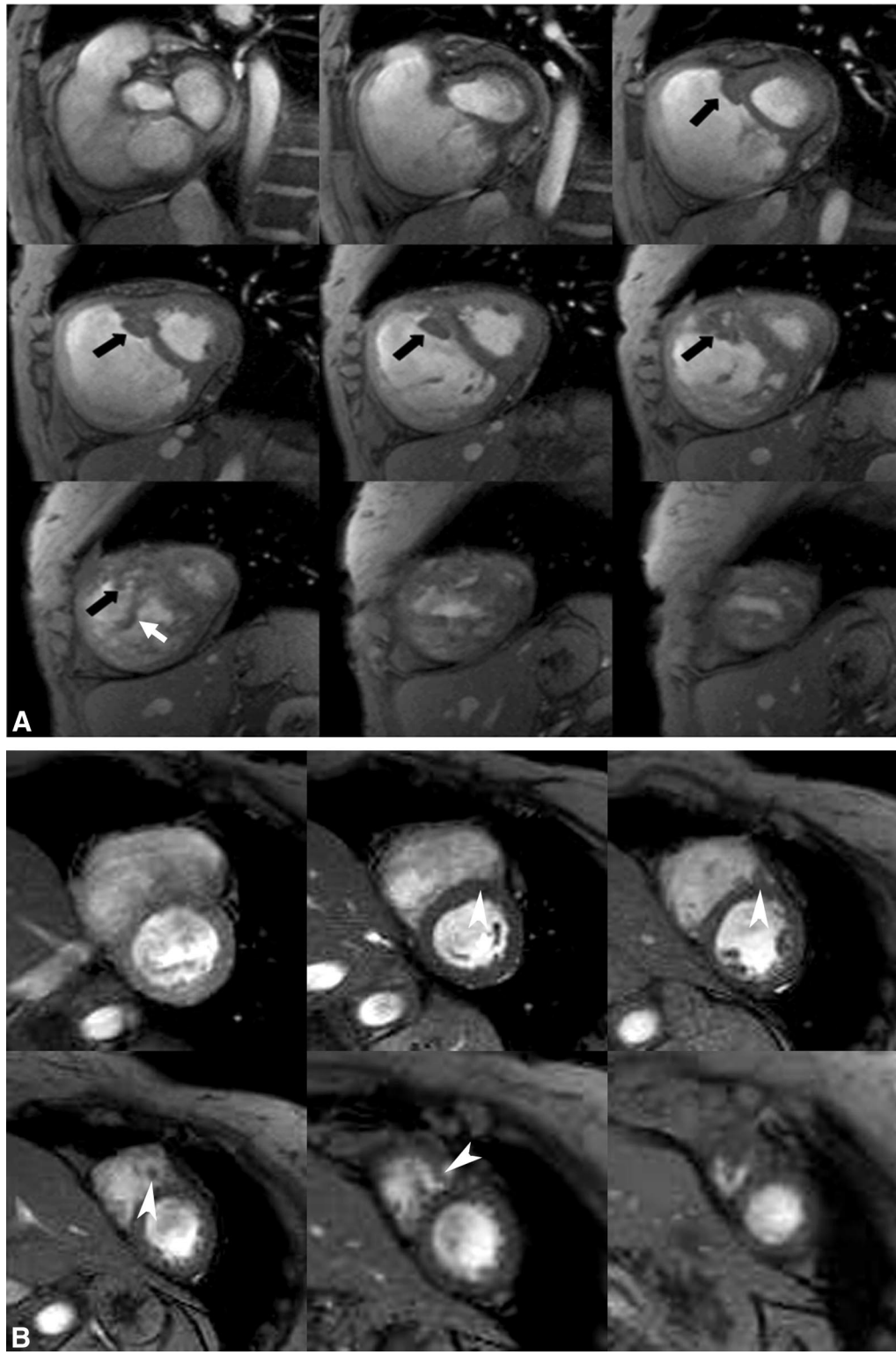

FIGURE 1. A, End-diastolic, short-axis turbo FLASH gradient echo cine MR images in a PH patient show hypertrophied SMT (black arrow) that arises from the interventricular septum (IVS) at the lower segment of the crista supraventricularis, forming a functional unit with the moderator band inferiorly (white arrow). The SMT shows the most hypertrophy compared with the other RV trabeculations. B, End-diastolic, short-axis turbo FLASH gradient echo cine MR images show normal SMT (white arrowheads) in a patient with scleroderma and absence of PH, as documented by RHC. C, The SMT mass can be easily assessed using dedicated software.

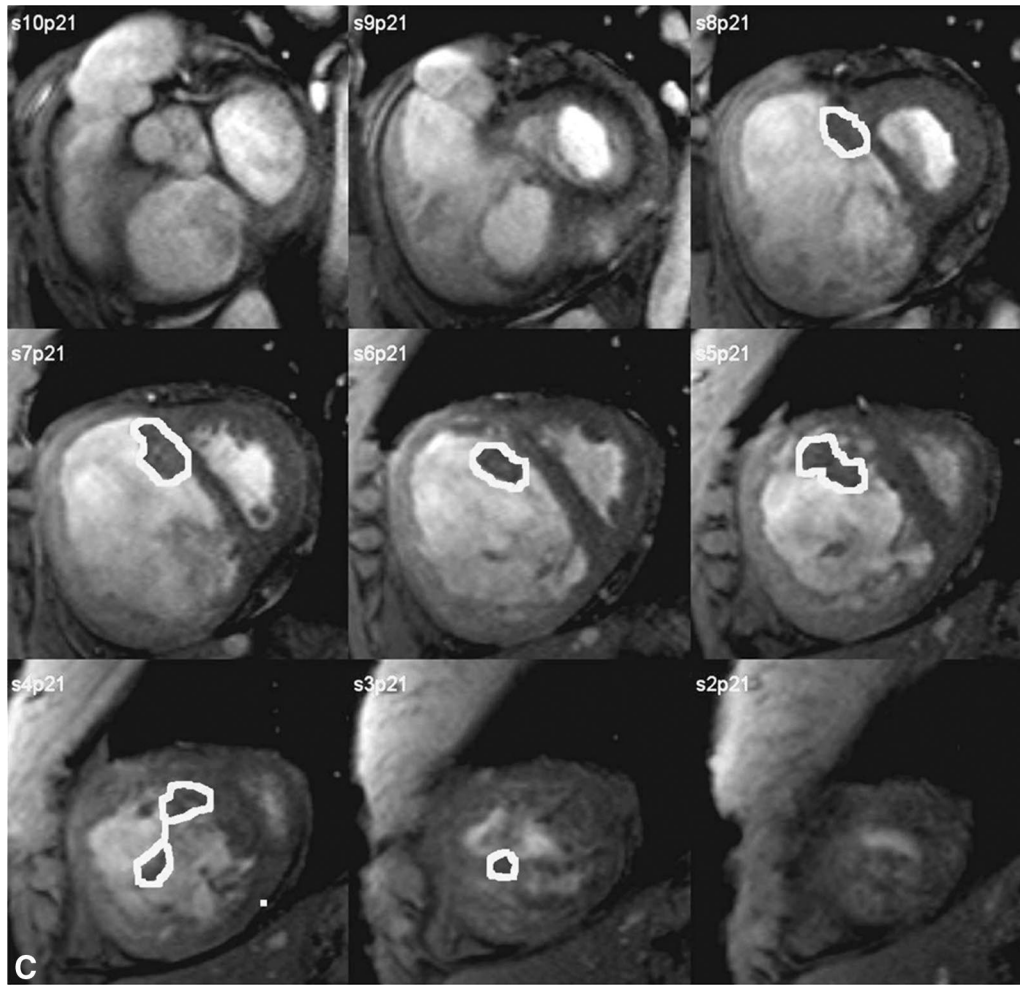

FIGURE 1. (*Continued*).

was approved by the Institutional Review Boards at both institutions. Written, informed consent was obtained from all participants. Exclusion criteria from our study were contraindications to MRI, incomplete MRI examination, or nondiagnostic MR image quality. Two patients were excluded because of breathing artifacts and cardiac arrhythmias that substantially affected cardiac MR image quality. Thus, the study sample consisted of 49 patients, 32 to 81 years of age (median: 64, 52–70) and included a larger proportion of women (n = 35 [71%]) (Table 1), reflecting a known higher prevalence of this disease in females.[18] The group consisted of 40 patients with PH (19 IPAH, 16 scleroderma-associated PAH, and 5 pulmonary venous hypertension) and 9 patients with suspected, but no PH. Based on the hemodynamic measurements, the patients were then divided into the following 2 groups: no PH (n = 9) and PH (mean pulmonary artery pressure [mPAP]: >25 mm Hg, n = 40).[19] At the time of the MRI examination and RHC, 14 out of the 40 PH patients (35%) were on one or more PH specific therapy (13 on phosphodiesterase inhibitors, 7 on prostacyclins, and 2 on endothelin receptor antagonists). One of the 9 patients (11%) with suspected, but no PH at RHC was on a phosphodiesterase inhibitor and on an endothelin receptor antagonist therapy (Table 1). This scleroderma patient had been diagnosed with PH by RHC 5 years previously (mPAP: 27 mm Hg). However, at repeat RHC for this study the mPAP was 20 mm Hg and he was, therefore included in the suspected, but no PH group. In addition, 18 healthy volunteers underwent MRI imaging at 3 Tesla (T) using the same imaging protocol as for patients; however, the volunteers were not subjected to RHC. These individuals were carefully screened for potential causes of PH as exclusion criteria. A lipid profile was also obtained, and the Framingham risk score was calculated. Other exclusion criteria for this control group were diabetes, smoking, hypertension, and a Framingham 10-year risk of cardiac disease >10%. The 18 control subjects were 41 to 69 years old (median: 49, 44–56) and included a larger proportion of women (n = 12 [67%]) (Table 1). Although these patients lacked confirmatory RHC data, they were assumed to be free of PH for the purpose of analysis.

MR Imaging

Imaging was performed at 2 centers, one using a 3T (Siemens Medical Systems, Germany) and the other using a 1.5T MR (Philips, The Netherlands) system. A series of parallel short-axis image planes (that encompassed the entire LV from the base to the apex) were acquired during short breath-holds using a retrospective electrocardiographically gated turbo FLASH segmented gradient echo (GRE) sequence at 3T and a steady-state free precession (SSFP) sequence at 1.5T. SSFP cine images were acquired using 3.2/1.6 (repetition time, milliseconds/echo time milliseconds), a high flip angle (60–90 degrees), and a bandwidth of 900 to 1000 Hz/pixel. Segmented gradient echo turbo FLASH cine images were acquired using 5.7/3.2 (repetition time milliseconds/echo time milliseconds),

TABLE 1. Patient Population

Final Diagnosis	Confirmed PH	Suspected But No PH	Controls
No. patients	40	9	18
Median age (25th, 75th)	64.5 (51.7, 70.8)	59 (53, 63)	49.0 (43.5, 55.5)*
Female	28	7	12
On medical therapy for PH	14 (35%)	1 (11%)	—
RHC			
mPAP (mm Hg)	45.0 (39, 52.5)	17.0 (15.0, 18.0)†	—
System PAP (mm Hg)	80.0 (62.0, 86.0)	29.0 (27.0, 30.0)†	—
PCWP (mm Hg)	10.0 (7.5, 12.0)	7.0 (6.0, 8.0)†	—
PVRI (Dyne s/cm^5/m^2)	850 (423, 1147)	228 (214, 282)†	—
CI (L/min × m^2)	2.3 (2.0, 3.0)	4.7 (4.2, 5)	—
MRI			
LV mass/BSA (g/m^2)	56.1 (50.8, 62.7)	70.0 (58.9, 74.6)†	69.4 (65.6, 80.3)
LVED volume/BSA (mL/m^2)	54.5 (45.1, 66.7)	60.8 (55.9, 67.6)	67.6 (59.5, 76.3)
LVES volume/BSA (mL/m^2)	17.9 (12.5, 23.4)	25.0 (18.3, 28.8)	23.3 (16.6, 29.3)
LVEF (%)	67.7 (60.0, 71,8)	58.2 (55.9, 68.9)	66.0 (59.9, 72,0)
RVED volume/BSA (mL/m^2)	84.9 (76.2, 99.4)	71.4 (63.5, 85.2)	76.0 (70.6, 86.2)
RVES volume/BSA (mL/m^2)	43.4 (37.1, 66.5)	32.4 (24.3, 44.8)	33.9 (27.2, 41.5)
RV stroke volume/BSA (mL/m^2)	35.4 (30.8, 40.3)	39.1 (35.7, 41.3)	43.6 (38.5, 47.0)
CI (L/min × m^2)	2.6 (2.1, 3.0)	3.0 (2.8, 3.3)†	3.0 (2.8, 3.5)
RVEF (%)	44.0 (32.1, 51.2)	54.7 (48.5, 56.6)†	54.5 (52.6, 61.5)
RV mass/BSA (g/m^2)	32.3 (24.7, 42.5)	19.7 (17.9, 28.4)†	25.5 (21.5, 28.7)
SMT mass (g)	4.5 (2.6, 6.6)	1.3 (0.96, 2.1)†	1.3 (0.83, 1.7)
SMT mass/BSA (g/m^2)	2.5 (1.5, 3.8)	0.79 (0.64, 1.3)†	0.66 (0.44, 0.92)
VMI	0.56 (0.42, 0.74)	0.34 (0.29, 0.38)†	0.34 (0.31, 0.40)

*$P < 0.05$ for the comparison with controls and suspected but absent PH. Displayed are median values with 25th and 75th percentile values.

†$P < 0.05$ for the comparison with confirmed PH and suspected but absent PH.

PH indicates pulmonary hypertension; mPAP, mean pulmonary artery pressure; systPAP, systolic pulmonary artery pressure; CI, cardiac index; PVRI, pulmonary vascular resistance index; PCWP, pulmonary capillary wedge pressure; RV, right ventricle; ED, end-diastolic; ES, end-systolic; BSA, body surface area; EF, ejection fraction; SMT, septomarginal trabeculation; LV, left ventricle; VMI, ventricular mass index.

a flip angle of 15 degrees, a bandwidth of 260 Hz/pixel, an acceleration factor of 2 Generalized Autocalibrating Partially Parallel Acquisition (GRAPPA), and 7 segments. Both MR systems had an 8-mm section thickness, a matrix of 256 ×192, a minimal field of view, a spatial resolution of 1.5 × 1.5 mm (typical), an acquired temporal resolution of 40 milliseconds, and 30 reconstructed cardiac phases.

Right Heart Catheterization

In all patients, RHC was performed with fluoroscopic guidance through the right internal jugular vein using a 4-lumen thermodilution catheter and a multiparameter monitor. Mean (end-expiratory) right atrial, pulmonary capillary wedge (PCWP), and pulmonary arterial pressures were recorded, and thermodilution cardiac output (CO) was obtained and reported as the average of at least 3 values with <20% variation. Heart rate and noninvasive blood pressure were recorded during the procedure. CO, cardiac index, and pulmonary vascular resistance (PVR = [mPAP − PCWP]/CO) were calculated. All patients completed the RHC procedure without complications. The diagnosis of pulmonary arterial hypertension (PAH) was defined as mPAP >25 mm Hg and PCWP of ≥15 mm Hg.[20] Patients with PH and PCWP >15 mm Hg were included (n = 5) and were classified as having pulmonary venous hypertension.

MR Imaging Analysis

End-diastolic cine frames were analyzed using MASS 6.2.1 software (Medis, the Netherlands). Starting from the basal slices, the SMT was identified in patients and controls as the most anterior trabeculation arising from the IVS below the outflow tract level (Fig. 1). One experienced observer (3 years of cardiac MRI experience), blinded to the patients' diagnosis and results of RHC, manually contoured and traced the SMT from its origin toward the apex, where the moderator band and secondary trabeculation arise (Fig. 1C). For interobserver agreement, a second-blinded experienced observer (2 years of cardiac MRI experience) manually contoured the SMT. Epicardial and endocardial ventricular borders were semi-automatically contoured for quantification of ventricular mass and functional indices. Papillary muscles and trabeculations in the LV and RV were excluded from the endocardial ventricular border definition and were included in the ventricular volume. End-diastolic and systolic volumes were defined visually. Stroke volume was calculated by subtraction of end-diastolic volume (EDV) from end-systolic volume (ESV). Ejection fraction (EF) was calculated as EF = stroke volume/EDV × 100. End-diastolic SMT mass, RV, and LV mass were measured according to the following equation: ventricular mass = 1.05 × (epicardial volume − endocardial volume). The IVS was excluded from the RV mass and included in the LV mass. The VMI was calculated from the RV and LV mass in diastole: VMI = RV mass/LV mass.

Statistical Analyses

Results are presented as median values with 25th and 75th percentile values. Ventricular mass and volume parameters were adjusted to body surface area (BSA; BSA (m^2) = 0.007184 ×

weight (kg) 0.425 × height (cm) 0.725). The Mann-Whitney *U* test was used for direct comparisons. The correlation between SMT mass and MR-derived cardiac functional indices, as well as catheter-derived hemodynamic parameters, was tested using Spearman rho correlation. A $P < 0.05$ was considered significant, and multiple comparisons were corrected for using the Bonferroni method. By using receiver operating characteristic (ROC) curves, SMT mass/BSA, VMI, and RV mass/BSA were analyzed for performance in the detection of PH. Multiple logistic regression models were analyzed to determine the association between SMT mass/BSA and the presence of PH, as defined by mPAP >25 mm Hg. A second logistic regression model included SMT mass/BSA, RV mass/BSA, LV mass/BSA, and gender. This model was developed to determine which measure of ventricular mass predicted PH status, while adjusting for gender. Inter-/intraobserver agreement was tested using the concordance correlation coefficient, Bland Altman plot with Pitman test of difference in variance. Comparison of correlation coefficients of the 1.5T and 3T subgroups was performed by computing the *Z* test for the equality of the 2 correlations after Fisher *r*-to-*Z* transformation. Statistical analyses were performed using STATA Statistical Software, version 10 (College Station, TX, 2008).

RESULTS

SMT Mass and PH

The SMT moderator band complex was identified in all participants on the short axis MR images. The SMT mass/BSA was significantly larger in the patients with PH (median, 2.5 g/m^2; 1.5–3.8) compared with the patients with suspected, but no, PH (median, 0.8 g/m^2; 0.6–1.4; Bonferroni corrected $P = 0.0032$; Table 1). There was no significant difference in SMT mass/BSA between the group with suspected but no PH and the control group (Bonferroni corrected $P = 1$). There was a significant positive correlation of SMT mass/BSA with the mPAP ($r = 0.62$, $P < 0.0001$) and pulmonary vascular resistance index (PVRI) ($r = 0.59$, $P < 0.0001$) (Table 2).

The area under the ROC curve (AUC) for SMT mass/BSA in diagnosing the presence or absence of PH was 0.84 (95% confidence interval [CI]: 0.75–0.96). When the control group was included in the analysis, the AUC was 0.88 (95% CI: 0.79–0.96) (Tables 3 and 4, Figs. 2A, B).

VMI and PH

VMI correlated well with the mPAP ($r = 0.72$, $P \leq 0.0001$) and PVRI ($r = 0.62$, $P \leq 0.0001$, Table 5). The AUC for the VMI in diagnosing the presence or absence of PH was 0.91 (95% CI: 0.82–0.99). When the control group was included in the analysis, the AUC was 0.87 (0.79–0.96) (Tables 3 and 4; Figs. 2A, C).

There was a significant difference in VMI between the group with suspected but no PH and the PH group (Bonferroni corrected $P = 0.0004$). There was no significant difference in VMI between the group with suspected but no PH and the control group (Bonferroni corrected $P = 1$, Table 1).

RV Mass and PH

The AUC for RV mass/BSA in diagnosing the presence or absence of PH was 0.78. When the control group was included in the analysis, the AUC was 0.73 (95% CI: 0.62–0.86) (Fig. 2). There was no significant difference in the AUC when comparing SMT mass/BSA, RV mass/BSA, and VMI ($P = 0.14$; $P = 0.50$ with controls).

SMT Mass, VMI, and RV Mass Correlation With RV Function and RHC

There was a significant positive correlation between SMT mass and RV mass, RV end systolic volume, RV end diastolic volume, and the VMI (Table 2). There was a significant inverse correlation between SMT mass and the RV EF and RV stroke volume (Table 2). There were significant correlations between VMI and RV mass with RV function parameters and RHC measurements (Tables 5 and 6).

TABLE 2. SMT Mass Correlations With MRI-Derived RV Function Parameters and RHC-Derived Hemodynamic Parameters

	Without Controls (n = 49)		With Controls (n = 67)	
SMT Mass/BSA Correlation With	***r***	***P***	***r***	***P***
RHC				
mPAP	0.62	<0.0001	—	—
systPAP	0.63	<0.0001	—	—
CI	−0.43	0.002	—	—
PVRI	0.59	<0.0001	—	—
PCWP	0.18	0.23	—	—
MRI				
RVED volume/BSA	0.35	0.01	0.29	0.02
RVES volume/BSA	0.50	<0.0001	0.48	<0.0001
RV stroke volume/BSA	−0.53	<0.0001	−0.61	<0.0001
RVEF %	−0.67	<0.0001	−0.65	<0.0001
RV mass/BSA	0.51	<0.0001	0.44	<0.0001
VMI	0.65	<0.0001	0.61	<0.0001
CI	−0.53	<0.0001	−0.58	<0.0001
LV mass/BSA	−0.22	0.12	−0.38	0.002
LVED volume/BSA (mL/m^2)	−0.45	0.001	−0.48	<0.0001
LVES volume/BSA (mL/m^2)	−0.33	0.02	−0.32	0.008
LVEF (%)	0.07	0.63	0.02	0.85

mPAP indicates mean pulmonary artery pressure; systPAP, systolic pulmonary artery pressure; CI, cardiac index; PVRI, pulmonary vascular resistance index; PCWP, pulmonary capillary wedge pressure; RV, right ventricle; ED, end-diastolic; ES, end-systolic; BSA, body surface area; EF, ejection fraction; SMT, septomarginal trabeculation; LV, left ventricle; VMI, ventricular mass index; RHC, right heart catheterization.

TABLE 3. Performance of SMT Mass, VMI, and RV Mass in Diagnosing the Presence or Absence of PH

Number	Parameter	AUC (95% CI)
67 (with controls): PH = 40, no PH = 27	SMT mass (g)/BSA	0.88 (0.79–0.96)
	VMI	0.87 (0.79–0.96)
	RV mass (g)/BSA	0.73 (0.62–0.85)
49 (without controls): PH = 40, no PH = 9	SMT mass (g)/BSA	0.84 (0.73–0.95)
	VMI	0.91 (0.82–0.99)
	RV mass (g)/BSA	0.78 (0.64–0.92)

PH indicates pulmonary hypertension; AUC, area under the receiver operating curve; SMT, septomarginal trabeculation; BSA, body surface area; VMI, ventricular mass index; RV, right ventricle.

SMT Mass, VMI, and RV Mass as Predictors of PH

Both SMT mass/BSA ($P = 0.005$, odds ratio: 8.6, 95% CI: 1.9–38.0) and VMI ($P = 0.012$, odds ratio: 1.1, 95% CI: 1.0–1.2) were found to be significant, independent predictors of PH in a logistic regression model that included VMI, SMT mass/BSA, and gender as parameters.

In the second step, we modified the above model and replaced VMI with RV mass/BSA and LV mass/BSA as parameters to

TABLE 4. Performance in Diagnosing the Presence or Absence of PH at Specific Cut Points

Number	Parameter	Cut Point	Sensitivity % (95% CI)	Specificity % (95% CI)	Correctly Classified in %
67 (with controls): PH = 40, no PH = 27	SMT mass (g)/BSA	1.3	83 (67–93)	85 (66–96)	84
	VMI	0.41	85 (70–94)	85 (66–96)	85
	RV mass (g)/BSA	26.5	70 (53–83)	63 (42–81)	67
49 (without controls): PH = 40, no PH = 9	SMT mass (g)/BSA	1.4	78 (62–89)	78 (40–97)	78
	VMI	0.41	85 (70–94)	89 (66–100)	88
	RV mass (g)/BSA	23.1	80 (64–91)	66 (30–93)	78

PH indictes pulmonary hypertension; AUC, area under the receiver operating curve; SMT, septomarginal trabeculation; BSA, body surface area; VMI, ventricular mass index; RV, right ventricle.

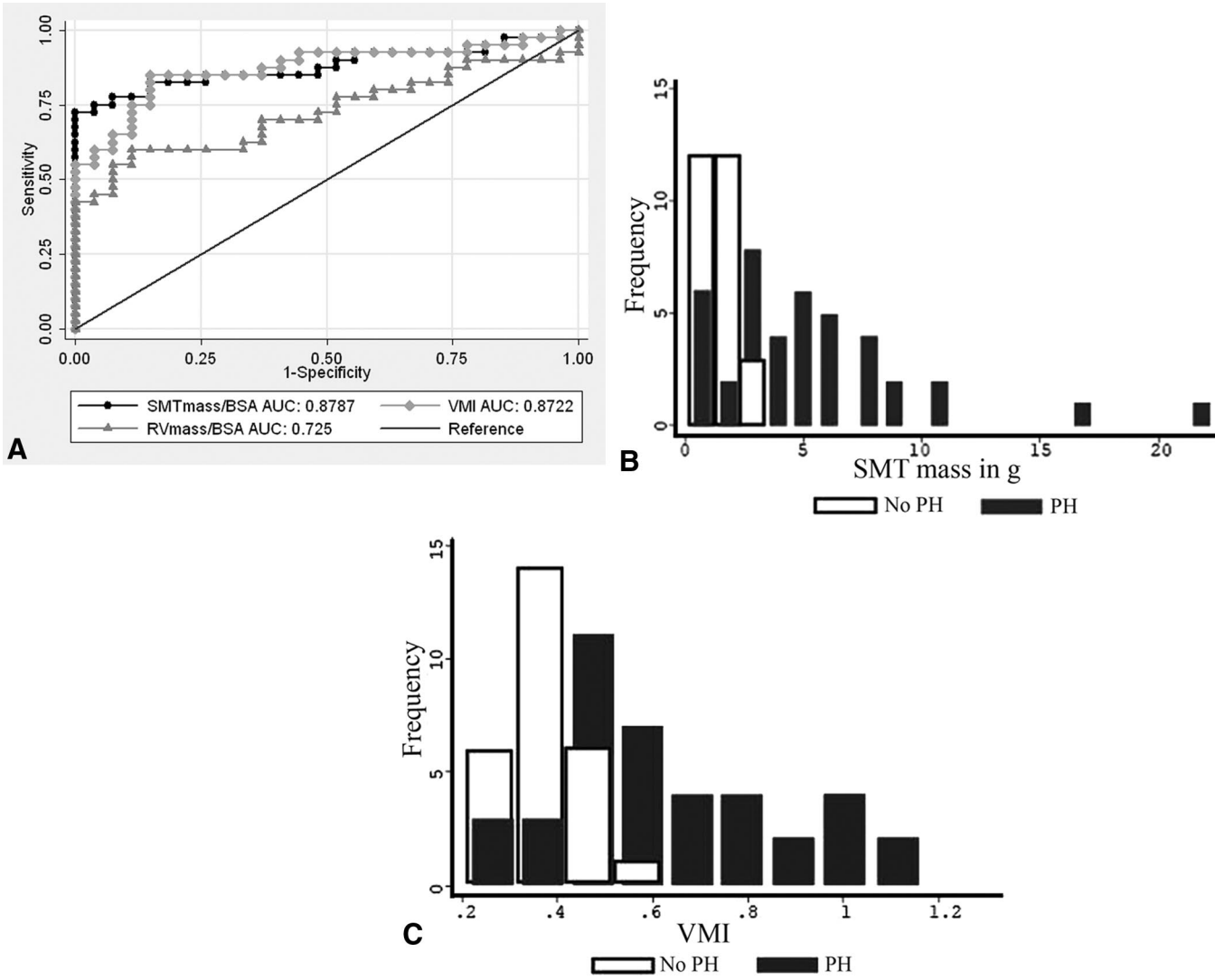

FIGURE 2. A, Receiver operating characteristic (ROC) curve shows the SMT mass/BSA and VMI to have good diagnostic accuracy in detecting the absence or presence of PH (mPAP, >25 mm Hg). There was no significant difference in the area under the curve between SMT mass/BSA, VMI, and RV mass/BSA, respectively, but there was a trend toward a lower AUC of the RV mass (A). Histogram analysis of SMT mass (in gram) and VMI show the differences between the PH and no PH groups (B, C).

determine whether the RV or LV mass was a predictor of PH. SMT mass/BSA (P = 0.017, odds ratio: 7.5, 95% CI: 1.4–38.8), RV mass/BSA (P = 0.018, odds ratio: 1.2, 95% CI: 1.0–1.4), and LV mass/BSA (P = 0.010, odds ratio: 0.9, 95% CI: 0.8–1.0) were found to be significant, independent predictors of PH in a logistic regression model.

TABLE 5. VMI Mass Correlations With MRI-Derived RV Function Parameters and RHC-Derived Hemodynamic Parameters

	Without Controls (n = 49)		With Controls (n = 67)	
VMI Mass Correlation With	***r***	***P***	***r***	***P***
RHC				
mPAP	0.72	<0.0001	—	—
systPAP	0.67	<0.0001	—	—
CI	−0.48	0.001	—	—
PVRI	0.62	<0.0001	—	—
PCWP	0.28	0.05	—	—
MRI				
RVED volume/BSA	0.55	0.001	0.39	0.001
RVES volume/BSA	0.68	<0.0001	0.51	<0.0001
RV stroke volume/BSA	−0.37	0.009	−0.48	<0.0001
RVEF %	−0.69	<0.0001	−0.59	<0.0001
RV mass/BSA	0.86	<0.0001	0.83	<0.0001
SMT mass/BSA	0.65	<0.0001	0.61	<0.0001
CI	−0.44	0.002	−0.47	<0.0001
LV mass/BSA	−0.22	0.12	−0.37	0.002
LVED volume/BSA (mL/m^2)	−0.39	0.006	−0.49	<0.0001
LVES volume/BSA (mL/m^2)	−0.37	0.01	−0.47	<0.0001
LVEF (%)	0.17	0.24	0.27	0.03

mPAP indicates mean pulmonary artery pressure; systPAP, systolic pulmonary artery pressure; CI, cardiac index; PVRI, pulmonary vascular resistance index; PCWP, pulmonary capillary wedge pressure; RV, right ventricle; ED, end-diastolic; ES, end-systolic; BSA, body surface area; EF, ejection fraction; SMT, septomarginal trabeculation; LV, left ventricle; VMI, ventricular mass index; RHC, right heart catheterization.

TABLE 6. RV Mass Correlations With MRI-Derived RV Function Parameters and RHC-Derived Hemodynamic Parameters

	Without Controls (n = 49)		With Controls (n = 67)	
RV Mass/BSA Correlation With	***r***	***P***	***r***	***P***
RHC				
mPAP	0.57	<0.0001	—	—
systPAP	0.55	<0.0001	—	—
CI	−0.30	0.04	—	—
PVRI	0.40	0.004	—	—
PCWP	0.34	0.02	—	—
MRI				
RVED volume/BSA	0.61	<0.0001	0.51	<0.0001
RVES volume/BSA	0.64	<0.0001	0.53	<0.0001
RV stroke volume/BSA	−0.13	0.36	−0.20	0.13
RVEF %/BSA	−0.57	<0.0001	−0.47	<0.0001
VMI	0.86	<0.0001	0.83	<0.0001
SMT mass/BSA	0.51	<0.0001	0.44	<0.0001
CI	−0.27	0.07	−0.26	0.03
LV mass/BSA	0.25	0.08	0.15	0.24
LVED volume/BSA (mL/m^2)	−0.22	0.14	−0.25	0.04
LVES volume/BSA (mL/m^2)	−0.28	0.06	−0.32	0.009
LVEF (%)	0.20	0.17	0.26	0.04

mPAP indicates mean pulmonary artery pressure; systPAP, systolic pulmonary artery pressure; CI, cardiac index; PVRI, pulmonary vascular resistance index; PCWP, pulmonary capillary wedge pressure; RV, right ventricle; ED, end-diastolic; ES, end-systolic; BSA, body surface area; EF, ejection fraction; SMT, septomarginal trabeculation; LV, left ventricle; VMI, ventricular mass index; RHC, right heart catheterization.

Inter- and Intraobserver Variability

The interobserver/intraobserver concordance with respect to the measurement of the SMT mass was high, with a concordance correlation coefficient of 0.95/0.98. The interobserver concordance for the measurement of the VMI, RV mass, and LV mass was also high, with concordance correlation coefficients of 0.97, 0.92, and 0.87, respectively (0.98, 0.98, and 0.96, respectively for intraobserver concordance). A Bland Altman analysis showed a mean SMT mass difference of −0.03 g (95% CI: 0.23/−0.30 g) between the 2 readers (Fig. 3). A Pitman test of difference in variance yielded an r of 0.053 with $P = 0.67$, showing no significant difference between the 2 readers.

The postprocessing time to analyze SMT mass (0.9 minutes; 95% CI: 0.7–1.2) was significantly shorter compared with the VMI postprocessing time (9.9 minutes; 95% CI: 9.2–10.6; $P < 0.0001$).

3T and 1.5T Patient Population Subanalysis

A subanalysis for all patients (n = 31), who underwent the 3T turbo FLASH cine MRI protocol showed no significantly different correlations with all measured RHC indices and biventricular functional measurements compared with the 1.5T patient cohort (n = 19). A separate ROC analysis for all patients and controls who underwent the 3T turbo FLASH cine MRI (n = 49) protocol did not show any significant differences in AUC values for the detection of PH when compared with the total patient group (AUC: 0.84 for VMI; 0.85 for SMT mass/BSA; and 0.72 for RV mass/BSA).

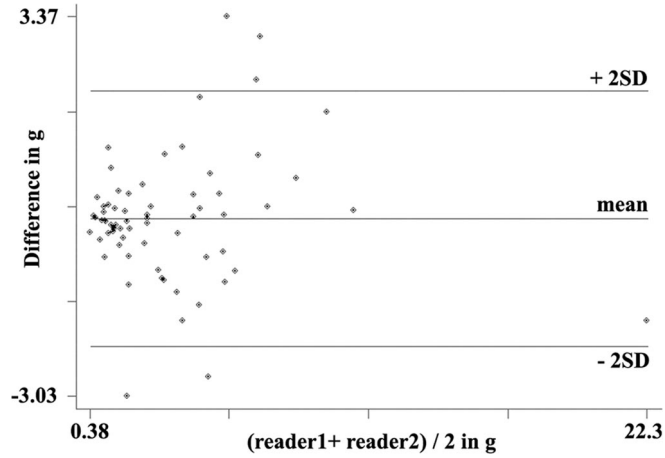

FIGURE 3. Bland Altman plot of reader 1 and reader 2 SMT mass reading. SD indicates standard deviation.

DISCUSSION

In this study, we prospectively measured the SMT mass using cardiac MR imaging in a group of consecutive patients with known or suspected PH. Using hemodynamic findings obtained by RHC performed within hours of the imaging studies, we demonstrate that cardiac MR-derived SMT mass measurement is a novel and reproducible marker of PH. Using ROC analysis, SMT mass and VMI had a similar performance in diagnosing the presence or absence of PH. Both SMT mass and VMI were found to be significant, independent predictors of PH. SMT mass is readily assessed by cardiac MRI and is, in our experience, significantly less time-intensive than

assessing VMI (less than a minute vs. 10 minutes for postprocessing time, respectively).

The measurement of SMT mass enabled identification of the presence or absence of PH with good accuracy, although the correlation of SMT mass with mPAP was not excellent ($r = 0.62$). The study group included individuals with PH of different etiologies, but essentially patients with IPAH and scleroderma-associated PAH as well as a few patients with pulmonary venous hypertension, which reflects the natural mixture of patients referred to our PH program for assessment of PH.

To our knowledge, this is the first study to systematically correlate the SMT mass assessed by MRI to invasive RHC findings in patients with known or suspected PH. Our study supports the hypothesis that the SMT-moderator complex functions not only as a conduction pathway, but also is involved in RV function mechanics. This complex appears to be an integral part of the RV remodeling process in PH, as suggested by significant correlations with RV mass and VMI parameters. We demonstrated that increased SMT mass correlated strongly with markers of RV dysfunction (Table 2): decreased RVEF and RV stroke volume and increased RVED and RVES volumes. Impaired RV function and more recently increased VMI have been linked to poor prognosis in patients with IPAH and scleroderma-associated PAH.[17,21–23] Future longitudinal studies will help determine whether increased SMT mass also predicts poor patient outcome.

The ability to diagnose PH using VMI tended to be superior compared with RV mass alone as a marker for PH, suggesting that the biventricular mass ratio is the most important factor in the detection of PH, compared with RV mass alone. This notion is supported by our findings that RV mass/BSA and LV mass/BSA are both independent predictors of PH. While RV mass/BSA had a significant positive correlation with mPAP ($r = 0.57$, $P < 0.0001$), LV mass/BSA tended to have a significant negative correlation with mPAP ($r = -0.28$, $P = 0.05$), the latter finding being most likely related to interventricular dependence as well as poor venous return resulting in chronic underfilling of the LV in PAH. This is supported by significant negative correlations of PVRI with LVED/BSA ($r = -0.59$, $P < 0.0001$), LVES/BSA ($r = -0.55$, $P < 0.0001$), and LV stroke volume/BSA ($r = -0.51$, $P = 0.0004$) in our patient population. These changes in opposite direction for RV mass/BSA and LV mass/BSA may explain why VMI tended to have a better performance than RV mass alone.

There are some limitations to our study. Thirty-one percent (15 of 49) of patients were on specific medical therapy for PH, which may have theoretically affected the remodeling of the SMT mass over time. Although there is very scant information on the effects of PH specific therapy on cardiac remodeling, sildenafil treatment has been shown to reduce RV mass and improve cardiac function over a period of 16 weeks.[24] However, since the majority of our patients was treatment naive, it is unlikely that therapy might have affected assessment of cardiac mass (including SMT or VMI) and our overall analysis.

For ethical reasons, asymptomatic control subjects did not undergo RHC measurements to confirm the absence of PH. However, it is unlikely that any of the control subjects had PH, given that IPAH is a rare disease with a prevalence of about 2 to 3 per million.[25] In addition, none of our controls had clinical conditions known to be associated with PH. Also, there were no significant differences in SMT mass or VMI in patients who were found not to have PH by RHC, compared with normal controls. Therefore, it is very unlikely that we might have included individuals with PH in the control group.

Another limitation of this study relates to the fact that 2 different MR systems (1.5T and 3T), sequences (SSFP and turbo FLASH GRE), and vendors were used. Small differences in RV and LV function parameters at 1.5T and 3T between the newer SSFP and the turbo FLASH GRE sequence have been reported.[26–28] However, there is improved blood pool-to-wall contrast and fewer artifacts at 3T, compared with 1.5T, with the turbo FLASH GRE sequence compared with the SSFP sequence.[29] Also a separate ROC subanalysis for all patients who underwent the 3T turbo FLASH cine MRI protocol did not show any significant differences when compared with the total cohort. Our VMI correlation with mPAP ($r = 0.72$) and performance to detect PH (AUC = 0.91) was similar to previously published data by Saba et al ($r = 0.81$,[9]) and Hagger et al ($r = 079$, AUC = 0.92,[17]) demonstrating the consistency of our results with the published literature using only one MR imaging technique.

In conclusion, we have identified in the MRI-derived measurement of SMT mass a novel, reproducible, and noninvasive marker of PH. VMI and SMT mass measurements by MRI were equally effective in detecting PH in our patient population, and both correlated well with indices of RV dysfunction. The value of SMT as a prognostic factor of outcome in PH and as a reliable end point for response to therapy needs to be further investigated in adequately designed longitudinal studies.

REFERENCES

1. D'Alonzo GE, Barst RJ, Ayres SM, et al. Survival in patients with primary pulmonary hypertension. Results from a national prospective registry. *Ann Intern Med*. 1991;115:343–349.
2. Simonneau G, Robbins IM, Beghetti M, et al. Updated clinical classification of pulmonary hypertension. *J Am Coll Cardiol*. 2009;54:S43–S54.
3. Yock PG, Popp RL. Noninvasive evaluation of intracardiac pressures using Doppler ultrasound: a case study of panvalvular regurgitation. *Clin Cardiol*. 1985;8:565–571.
4. Currie PJ, Seward JB, Chan KL, et al. Continuous wave Doppler determination of right ventricular pressure: a simultaneous Doppler-catheterization study in 127 patients. *J Am Coll Cardiol*. 1985;6:750–756.
5. Berger M, Haimowitz A, Van Tosh A, et al. Quantitative assessment of pulmonary hypertension in patients with tricuspid regurgitation using continuous wave Doppler ultrasound. *J Am Coll Cardiol*. 1985;6:359–365.
6. Arcasoy SM, Christie JD, Ferrari VA, et al. Echocardiographic assessment of pulmonary hypertension in patients with advanced lung disease. *Am J Respir Crit Care Med*. 2003;167:735–740.
7. Fisher MR, Forfia PR, Chamera E, et al. Accuracy of Doppler echocardiography in the hemodynamic assessment of pulmonary hypertension. *Am J Respir Crit Care Med*. 2009;179:615–621.
8. Pennell DJ, Sechtem UP, Higgins CB, et al. Clinical indications for cardiovascular magnetic resonance (CMR): consensus panel report. *J Cardiovasc Magn Reson*. 2004;6:727–765.
9. Saba TS, Foster J, Cockburn M, et al. Ventricular mass index using magnetic resonance imaging accurately estimates pulmonary artery pressure. *Eur Respir J*. 2002;20:1519–1524.
10. Dellegrottaglie S, Sanz J, Poon M, et al. Pulmonary hypertension: accuracy of detection with left ventricular septal-to-free wall curvature ratio measured at cardiac MR. *Radiology*. 2007;243:63–69.
11. Sanz J, Kuschnir P, Rius T, et al. Pulmonary arterial hypertension: noninvasive detection with phase-contrast MR imaging. *Radiology*. 2007;243:70–79.
12. Sanz J, Dellegrottaglie S, Kariisa M, et al. Prevalence and correlates of septal delayed contrast enhancement in patients with pulmonary hypertension. *Am J Cardiol*. 2007;100:731–735.
13. James TN. Anatomy of the crista supraventricularis: its importance for understanding right ventricular function, right ventricular infarction and related conditions. *J Am Coll Cardiol*. 1985;6:1083–1095.
14. Kilner PJ, Sievers B, Meyer GP, et al. Double-chambered right ventricle or sub-infundibular stenosis assessed by cardiovascular magnetic resonance. *J Cardiovasc Magn Reson*. 2002;4:373–379.
15. Rowland TW, Rosenthal A, Castaneda AR. Double-chamber right ventricle: experience with 17 cases. *Am Heart J*. 1975;89:455–462.
16. Shah A, Schwartz H, Class RN. Unusual echocardiographic findings in primary pulmonary hypertension. *Arch Intern Med*. 1983;143:820–822.
17. Hagger D, Condliffe R, Woodhouse N, et al. Ventricular mass index correlates with pulmonary artery pressure and predicts survival in suspected

systemic sclerosis-associated pulmonary arterial hypertension. *Rheumatology*. 2009;48:1137–1142.

18. Taichman DB, Mandel J. Epidemiology of pulmonary arterial hypertension. *Clin Chest Med.* 2007;28:1–22, vii.
19. Galie N, Manes A, Uguccioni L, et al. Primary pulmonary hypertension: insights into pathogenesis from epidemiology. *Chest*. 1998;114:184S–194S.
20. Simonneau G, Galie N, Rubin LJ, et al. Clinical classification of pulmonary hypertension. *J Am Coll Cardiol*. 2004;43:5S–12S.
21. van Wolferen SA, Marcus JT, Boonstra A, et al. Prognostic value of right ventricular mass, volume, and function in idiopathic pulmonary arterial hypertension. *Eur Heart J*. 2007;28:1250–1257.
22. Fisher MR, Mathai SC, Champion HC, et al. Clinical differences between idiopathic and scleroderma-related pulmonary hypertension. *Arthritis Rheum*. 2006;54:3043–3050.
23. Vonk Noordegraaf A, Naeije R. Right ventricular function in scleroderma-related pulmonary hypertension. *Rheumatology (Oxford)*. 2008;47(suppl 5): v42–v43.
24. Wilkins MR, Paul GA, Strange JW, et al. Sildenafil versus Endothelin Receptor Antagonist for Pulmonary Hypertension (SERAPH) study. *Am J Respir Crit Care Med*. 2005;171:1292–1297.
25. Gaine SP, Rubin LJ. Primary pulmonary hypertension. *Lancet*. 1998;352: 719–725.
26. Malayeri AA, Johnson WC, Macedo R, et al. Cardiac cine MRI: quantification of the relationship between fast gradient echo and steady-state free precession for determination of myocardial mass and volumes. *J Magn Reson Imaging*. 2008;28:60–66.
27. Hudsmith LE, Petersen SE, Tyler DJ, et al. Determination of cardiac volumes and mass with FLASH and SSFP cine sequences at 1.5 vs. 3 Tesla: a validation study. *J Magn Reson Imaging*. 2006;24:312–318.
28. Tyler DJ, Hudsmith LE, Petersen SE, et al. Cardiac cine MR-imaging at 3T: FLASH vs SSFP. *J Cardiovasc Magn Reson*. 2006;8:709–715.
29. Michaely HJ, Nael K, Schoenberg SO, et al. Analysis of cardiac function–comparison between 1.5 Tesla and 3.0 Tesla cardiac cine magnetic resonance imaging: preliminary experience. *Invest Radiol*. 2006;41:133–140.